Sediment entrainment and depletion from patches of fine material in a gravel-bed river

Damia Vericat,[1] Ramon J. Batalla,[2,3] and Chris N. Gibbins[4]

Received 26 March 2008; revised 3 July 2008; accepted 18 August 2008; published 12 November 2008.

[1] This paper presents the results of experiments in which a portable flume was used to manipulate hydraulic conditions and create bed load transport in a gravel bed river. Flume data are coupled with those from Helley-Smith samples to assess bed load characteristics at shear stresses ranging from 5 to 60 N/m^2. Experiments demonstrate that patches of fine sediment control both the intensity and duration of bed load under hydraulic conditions characteristic of the early stages of floods. The experiments allow quantifying bed load at the entrainment threshold, providing the first empirical evidence that marginal bed load transport can be attributed to the mobilization of sediments from patches. Bed load transport was recorded consistently once shear stress exceeded 5 N/m^2. The experiments produced low bed load rates (<6 g/sm). Depletion of material in the patches occurred rapidly, with bed load rates and particle sizes decreasing after only 5 minutes. Combining flume and Helley-Smith data for the study reach, a breakpoint in the relation between shear stress and bed load rate was calculated to be around 30 N/m^2. This represents the transition between bed load transport phases: below the breakpoint, transport occurs at a low rate and is composed predominantly of fine sediment from patches, but above it, much higher rates occur from across the reach as a whole. Hydraulic conditions at the threshold are those which occur during small, frequent floods (25% bankfull, flow equaled or exceeded 15% of time). This indicates that sediment entrainment from patches of fine material is a frequent process and the threshold change between bed load phases occurs regularly.

Citation: Vericat, D., R. J. Batalla, and C. N. Gibbins (2008), Sediment entrainment and depletion from patches of fine material in a gravel-bed river, *Water Resour. Res.*, *44*, W11415, doi:10.1029/2008WR007028.

1. Introduction

[2] Patches of fine material play an important role in sediment transport in gravel bed rivers [*Garcia et al.*, 1999; *Laronne et al.*, 2001]. The term "patch" was used initially in terrestrial and marine environmental studies [*Wiens*, 1976] but later adopted by fluvial geomorphologists to describe an aggregation of homogeneous bed sediment. In rivers and streams, patches of fine sediment occupying areas less than 1 m^2 have been termed "micropatches" [*Laronne et al.*, 2001; *Church and Hassan*, 2005]. These typically occur in depressions on bar surfaces or behind obstacles such as large cobbles and are considered to be a readily available source of sediment in gravel bed rivers [*Mosley and Tindale*, 1985]. They are particularly important in contributing to bed load in the early stages of flood events and may be the dominant source of material transported during small and medium sized events.

[3] A number of authors have reported two distinct phases of bed load transport in gravel- and cobble-bed rivers [*Jackson and Beschta*, 1982; *Carling*, 1988; *Ryan et al.*, 2002]. In *Phase I* only small quantities of sands and fine gravels are mobilized from the bed, while in *Phase II* larger quantities and a broader range of size classes are entrained. Because of flood magnitude/frequency relations, *Phase II* is less frequent than *Phase I*. Although during a given hydrological event the threshold change between phases may be difficult to define [*Ryan et al.*, 2002], *Phase II* has been documented to occur near bankfull discharge [*Parker et al.*, 1982; *Andrews*, 1984; *Andrews and Nankervis*, 1995].

[4] *Ashworth and Ferguson* [1989] proposed a more complex classification which recognized three bed load transport phases. Unlike authors who reported two phases, *Ashworth and Ferguson* [1989] analyzed bed load transport during flood events with shear stresses up to 400 N/m^2 (i.e., high magnitude events). They argued that in the early stage of a flood hydrograph, only the sand fraction is transported (their *Phase I* bed load transport) but, as flow increases, size-selective entrainment occurs (their *Phase II*). During high flow events, equal mobility is reached and the entire range of bed particle sizes is entrained; this they classified as *Phase III*.

[5] The sources of sediment during low bed load transport conditions (*Phases I* and *II* as per *Ashworth and*

[1]Centre for Catchment and Coastal Research, Institute of Geography and Earth Sciences, Aberystwyth University, Aberystwyth, Wales, Ceredigion, UK.
[2]Department of Environment and Soil Sciences, University of Lleida, Lleida, Catalonia, Spain.
[3]Forestry and Technology Center of Catalonia, Solsona, Catalonia, Spain.
[4]Department of Geography and Environment, University of Aberdeen, Aberdeen, UK.

0043-1397/08/2008WR007028

Table 1. Phases Outlining Bed Material Entrainment and Transport in Gravel-Bed Rivers[a]

Source of Material[b]	*Jackson and Beschta* [1982]	Descriptor	*Ashworth and Ferguson* [1989]	Descriptor	*Garcia et al.* [2007]	Descriptor
PATCHES BED					*Phase I* →	within patch grain instability; no net bed load
					Phase II →	within patch gyratory step-and-rest motion; no net bed load
	Phase I →	small amount of sand and fine gravels mobilized	***Phase I*** →	only sand fraction transported	***Phase III*** →	general sediment motion from patches
			Phase II →	size-selective entrainment		
	Phase II →	larger quantities and almost all sizes classes transported	*Phase III* →	full river-bed mobility		

[a]In bold the areas addressed in this paper.
[b]Patch material: loose fine sediment, sand and fine gravels ($D_{50\text{-}p}$ = 1.2 mm). Bed material: armored, $D_{50\text{-}s}$ = 49 mm while $D_{50\text{-}ss}$ = 24 mm (see text for more details).

Ferguson [1989]) are those relatively small areas in the river bed where sands and fine gravels are stored following the most recent full mobility event [*Ryan et al.*, 2002]. Storage areas may be in pools where energy is dissipated and deposition occurs, or patches. Large clasts can cluster and so create small-scale bed forms [*Wittenberg*, 2002] which influence hydraulic conditions experience by material in patches. Larger clasts can reduce the hydraulic forces acting on smaller material [*Neill*, 1968]. This "hiding effect" has been identified as the main cause of the stability of fine particles when shear stress exceeds the theoretical value for their entrainment [e.g., *Egiazaroff*, 1965].

[6] Historically, Helley-Smith sampling has been the most frequently used technique for collecting bed load data. However, this technique may underestimate the quantity of fine material moving across the bed due, for example, to blockage or what has been termed "perching" [*Vericat et al.*, 2006]. There is also the more fundamental problem that, in order to characterize *Phase I* bed load transport, Helley-Smith sampling requires the operator to have the predictive capacity to be in place to sample the very early stages of flood events. Automated sampling devices such as Birkbeck pit-traps have been designed to overcome this problem and have provided important insights into bed load transport processes [*Reid et al.*, 1980]. However, because of their relatively high detection thresholds, the current generation of pit traps do not provide information during episodes of low bed load transport. Thus there remains a paucity of field data on low bed load transport conditions in gravel bed rivers.

[7] *Garcia et al.* [2007] present one of very few studies describing entrainment and low bed load transport from patches of fine material in upland, gravel bed rivers. Using video recordings, they observed how, as discharge increases, within-patch grain instability, followed by within-patch gyratory step-and-rest motion, followed in turn by general sediment motion, occur. *Gibbins et al.* [2007a, 2007b] used a novel portable flume to assess the relations between hydraulic conditions and the entrainment of both sediments and invertebrates from patches of fine material in a gravel bed river. Their flume allowed manipulation of conditions in situ, rather than in a laboratory flume setting where experimental artifacts can confound interpretation of geomorphological and ecological responses.

[8] Here we report observations of incipient bed load transport obtained by using this portable flume to increase shear stress over patches of fine material in a gravel bed river. Specific objectives of the experiments were (1) to characterize transport rates and the grain size distribution (GSD) of the bed load originating from patches of fine sediment, (2) to assess the influence of hiding on entrainment of patch material, and (3) to determine whether depletion of fine material occurs during low bed load events. We combine data from the experiments with those collected using a Helley-Smith sampler during natural flood events, when parts of the bed and, eventually, subsurface material across the entire study reach were mobilized. In this way we present an integrated assessment of the characteristics of, and controls on, bed load transported under a broad range of flow conditions. The entrainment phases dealt with in the paper are specified in Table 1.

2. Study Reach

[9] The study reach is located in the Ribera Salada, an unmodified upland gravel bed river in the northeast of the Ebro basin (Figure 1). The Ribera Salada is a tributary of the Segre River, which flows into the Rialb Reservoir. The Ribera Salada drains an area of 222 km^2, across which the mean annual precipitation is around 800 mm. *Batalla et al.* [2005] reported a median discharge of 1 m^3/s for the study reach, a main stem section located approximately in the center of the catchment (Figure 1).

[10] The flume experiments and Helley-Smith sampling were undertaken in a 150-m long reach with an average slope of 0.01. The reach consists of a succession of plane-bed and riffle-pool morphologies. Patches of sand and fine gravels are distributed across the reach and cover approximately 20% of its surface area [*Müller et al.*, 2008]. These are small (typically less than 1 m^2) and so fall into the micropatch category as described by *Laronne et al.* [2001] and *Church and Hassan* [2005].

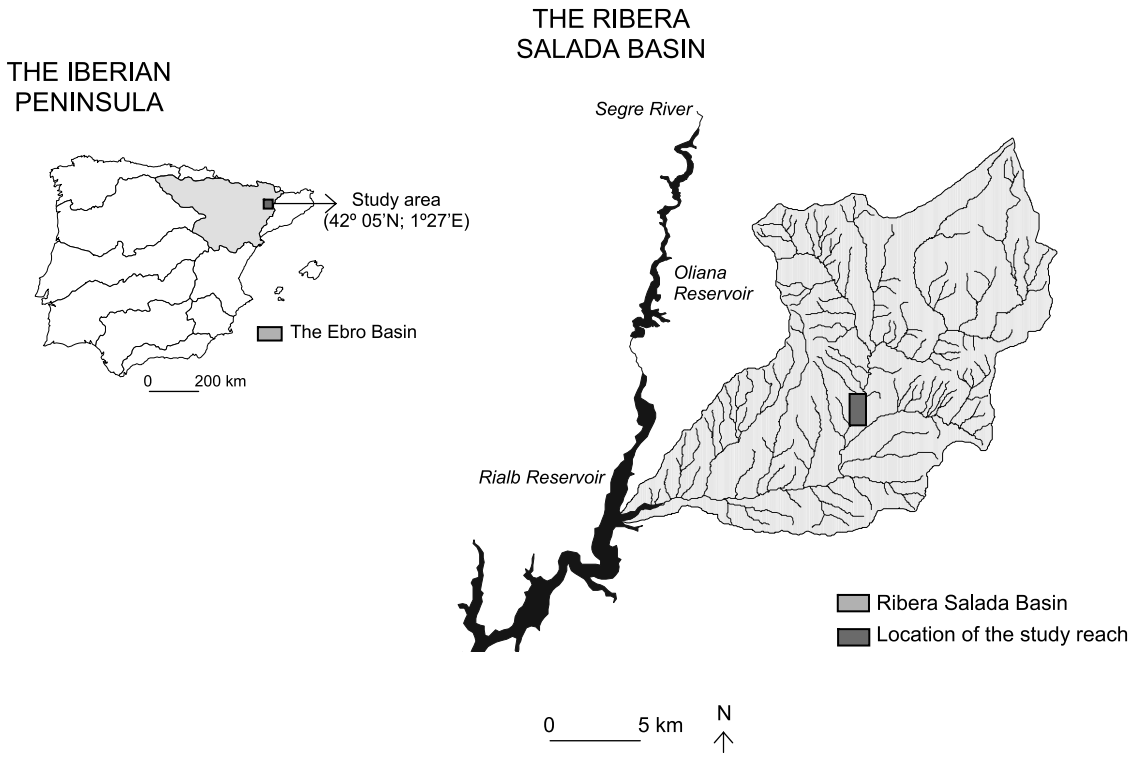

Figure 1. Location of the Ribera Salada river in the Iberian Peninsula and the study reach where flume experiments and bed load sampling were carried out.

[11] The grain-size characteristics of patches and their potential role in bed load transport in the reach were originally reported by *Batalla et al.* [2005] and recently used for model testing by *Müller et al.* [2008]. Surface and subsurface material across the reach were fully described by *Gibbins et al.* [2007b]. Sediments in the patches were sampled using the area by weight method (following methods described by *Kellerhals and Bray* [1971]). Surface material across the reach was characterized using 500 randomly selected particles, sized by passing them through a template with square holes scaled at ½ ϕ intervals [*Wolman*, 1954]. The subsurface material was sampled using the volumetric method [*Lane and Carlson*, 1953]. The total weight of the subsurface material sampled was 150 kg (1.7% of the largest subsurface particle weight), producing acceptable accuracy for the estimate of the subsurface grain size distribution [*Church et al.*, 1987]. Using these methods, the average median surface material ($D_{50\text{-}s}$) across the reach was calculated to be 49 mm, while the median subsurface size ($D_{50\text{-}ss}$) was 24 mm; 17% of the subsurface material was sand (Figure 2). The armoring ratio of the reach is 2, calculated as the ratio of the median surface and subsurface sizes (i.e., $A_r = D_{50\text{-}s}/D_{50\text{-}ss}$), indicating that the river bed is armored [*Bunte and Abt*, 2001]. The average median material ($D_{50\text{-}p}$) in the patches is 1.2 mm, with $D_{50\text{-}p}$ ranging from 0.6 to 2.2 mm; the percentage of sand in the patches varies from 30 to 62%.

3. Data and Methods

3.1. Equipment and Protocols

[12] The main set of bed load samples analyzed in this paper are those obtained by *Gibbins et al.* [2007a, 2007b] during invertebrate drift experiments using the portable flume (Figure 3a). These are complemented using Helley-Smith samples from the reach reported by *Batalla et al.* [2005]. The flume was designed to recreate the hydraulic conditions attained during the early stages of floods or those typical of high frequency/low magnitude events. The flume was large enough to encompass individual patches. When positioned over a patch with the flume doors in their normal position (parallel to main flume sides, as in the plate in Figure 3b) there was no manipulation of hydraulic conditions inside. As all experiments were conducted during a period of relatively low flows (always less than the median annual discharge), there was no bed load transport occurring naturally; thus it was necessary to manipulate hydraulics in order to initiate bed load transport. This was achieved by opening the flume doors, so as to funnel more water inside (as in the plate in Figure 3c). This increased depth (d), velocity (v), and shear stress (τ_b) over the targeted patch inside the flume. Further increases were achieved through the use of a Perspex sheet. The sheet slid vertically into position at the upstream end of the manipulated area of bed (the downstream end of the doors). Once fixed into position, it partially dammed the water entering the manipulated area. Water was forced under pressure through a 15-cm gap between the bottom of this sheet and the streambed; this produced a jet of water which increased near-bed velocity over each patch of fine material (see supplementary video file in *Vericat et al.* [2007] for more details).

[13] With the flume doors open, stream flow lines over the patch of channel were different to those prior to the flume being put in position. This alteration was essential in order to achieve threshold conditions for sediment entrainment. Flume walls were very thin (1 cm) and made of light,

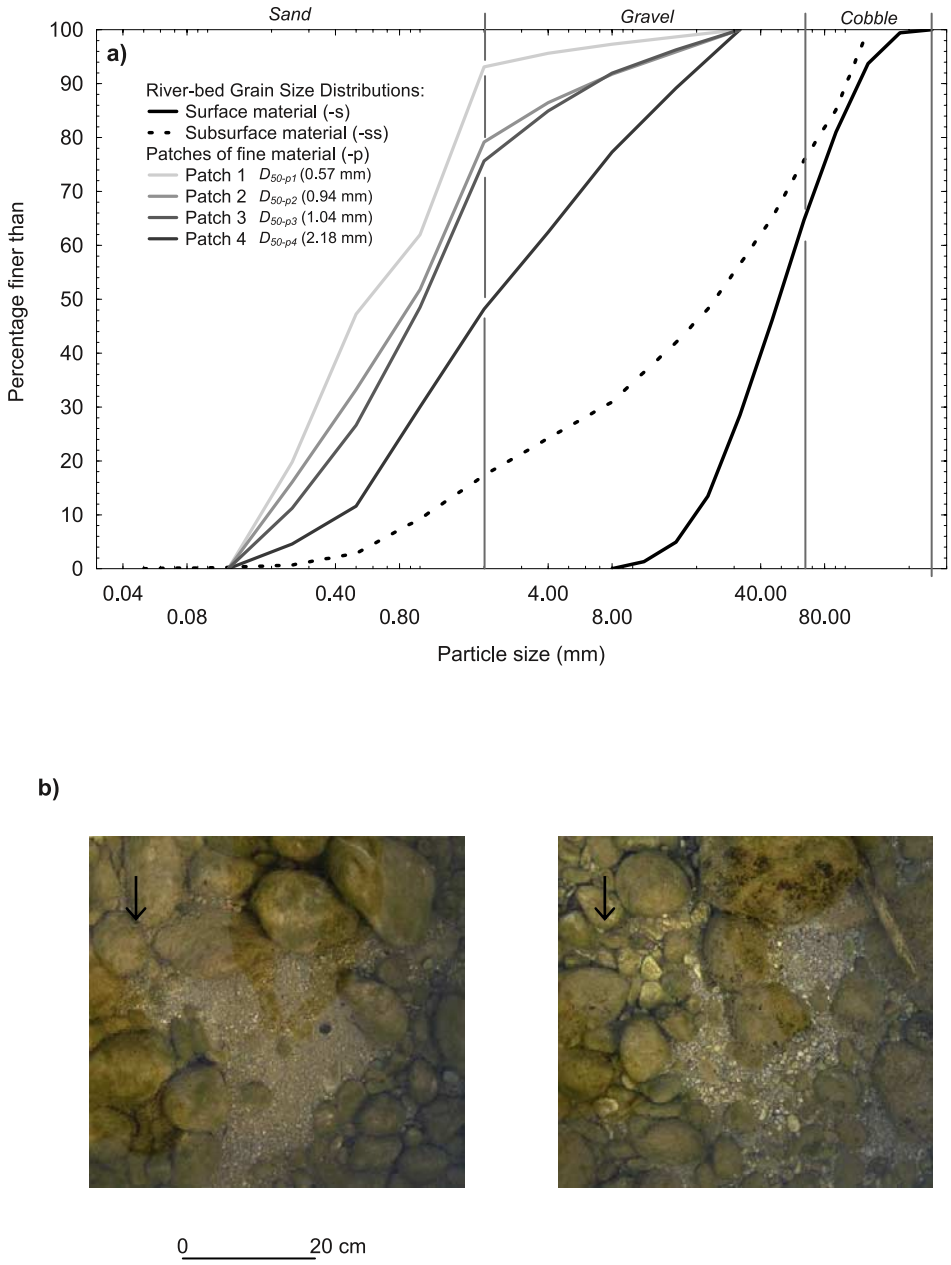

Figure 2. (a) River bed material grain size distributions. (b) Photographs of representative patches of fine material in the study reach.

smooth material (i.e., Perspex) to ensure minimum flow disturbance. Nevertheless, once doors were opened to their widest point, their angle could lead to eddy shedding, increasing near-bed turbulence over the patch. The walls also cut the transverse energy exchange, although no empirical data are available to allow us to assess these effects. The surface profile and the water depth within the 1-m long flume were very constant when the doors were open, suggesting that no flow acceleration occurred. Replicate velocity measurements were very similar (σ = 0.09 m/s) suggesting steady flow conditions. Thus we assume a steady flow state over each target patch during the flow manipulations.

[14] During each period of manipulation, velocity was measured by means a Valeport electromagnetic flowmeter (Model 801) at 0.4 $\times$ d and at 0.2 $\times$ d at the center point of the area of streambed encompassed by the flume. Velocity was measured over a 1-minute recording period. Because the Perspex sheet disrupted the vertical velocity profile inside the flume, it was invalid to calculate local shear stress using the velocity profile. Instead, the local boundary shear stress was calculated for each experiment using the formula and criteria used by *Whiting and Dietrich* [1990]:

$$\tau_b = \rho(v_z\ k)^2[\ln(10z/D_{84-s})]^{-2}$$

where τ_b is the local boundary shear stress in N/m^2, ρ is the fluid density (1000 kg/m^3), v_z is the flow velocity at height z above bed (in m/s), k is von Karman's constant (0.40), z is the height above bed (in m), and $D_{84\text{-}s}$ is the 84th percentile

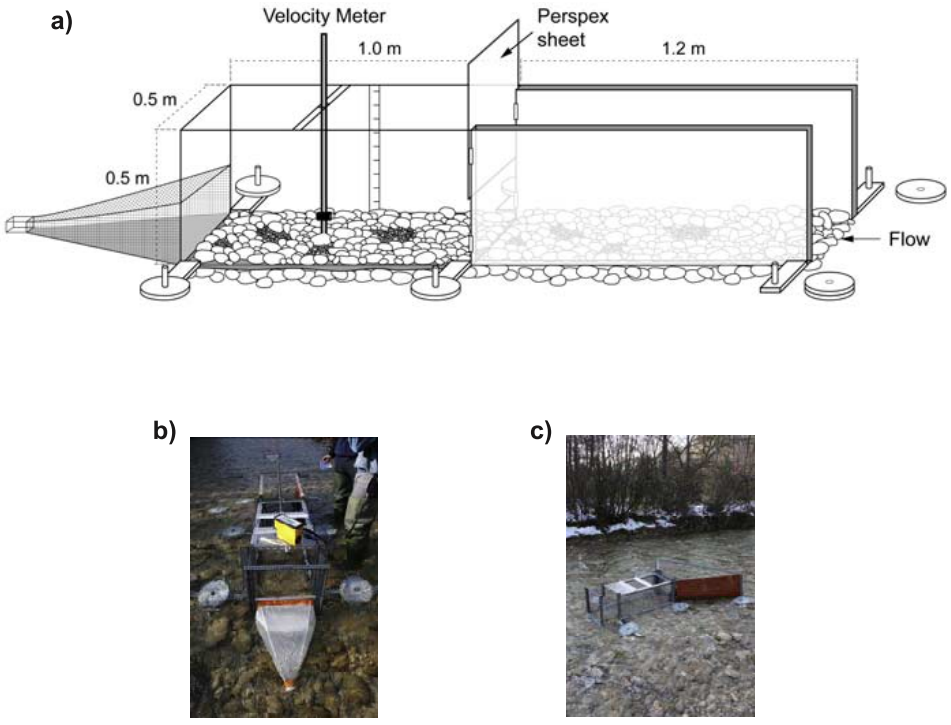

Figure 3. (a) Characteristics and dimensions of the portable flume used during for field experiments (modified from *Vericat et al.* [2007]). (b) Photograph of the flume showing doors in parallel (no manipulation). Shear stress on the targeted patches was increased by opening the hinged doors (c) and by sliding vertically in a Perspex sheet at the upstream end of the manipulated area of bed; see text and references for a complete description.

value (in m) 84 from the surface reach average grain size distribution.

[15] The equation is based on the law of the wall and the choice of roughness height is critical. z_0 is the point above the bed where velocity is projected to go to zero and is taken to be 0.1 times the reach $D_{84\text{-}s}$ sized material (i.e., equivalent sand roughness k_s is $3D_{84\text{-}s}$; e.g., *Limerinos* [1970]). *Robert et al.* [1992] reported how velocity profiles downstream from roughness transitions are significantly altered. Due to the spatial lag effect, the velocity profile over a patch of fine material is controlled by the roughness effects of the coarser upstream material. Our experiments were conduced in such roughness transitions: the transition between gravel-cobble protrusions and adjacent patches of finer material. Thus to accommodate the spatial lag of the velocity profile, we used the average reach $D_{84\text{-}s}$ instead of the patch D_{84} to derive the z_0. Sensitivity tests indicate that boundary shear stress estimates would be around 35% lower if patch D_{84} was used.

[16] Velocity measurements used for the shear stress calculations were made at $0.2 \times d$, fulfilling the recommendation of *Whiting and Dietrich* [1990]. *Whiting and Dietrich* [1991] used this formula in a stream where velocity conditions were similar to the flume (i.e., increased near bed velocity relative to that higher up in the water column).

[17] A standard invertebrate drift net (0.5 m wide, 0.25 m high, 0.5 m long, and 1 mm mesh diameter) was fixed to the downstream end of the flume (Figure 3) and this captured material mobilized from patches during periods of manipulation. The base of the net sat on the streambed. Sponge rubber fitted to the base ensured that, when fitted in place and pressed downward, there was little or no space between the base of the net and the bed. This helped minimize bed load passing under the net. At each experimental location, a drift net was placed in the channel 2 m upstream from the flume and left in position for the period of manipulation. This allowed assessment of any bed load transport occurring naturally in the reach during the experiments.

[18] Although the drift net mesh was 1-mm diameter, some material finer than this was retained. In order to avoid errors due to under-measurement of fine sand, bed load samples were truncated at 1 mm. The mean ratio between the untruncated and truncated bed load sample weights was 1.37 (σ = 0.30), indicating that calculated bed load rates were not markedly affected by truncation.

[19] Particulate organic matter was not a major component in the samples because experiments were conducted in the early spring, a time when there is very little particulate organic matter in the stream. Replicate velocity measurements during each experiment yield almost the same values, indicating that backwater effects due to progressive net clogging did not occur. Therefore we conclude that there is no concern over the potential clogging of the net by organic material.

3.2. Experimental Trials

[20] Experiments were conducted at 30 locations across the study reach. At each location, data from two contiguous 5-minute time periods were used to assess bed load dynamics. Velocity was measured during each period. Bed load samples were collected in the first 5-minute period of manipulation (flume doors opened) and used to assess rates of entrainment from patches (hereafter *Pent* samples). At the

end of this period, the drift net was removed, emptied and quickly (<30 seconds) replaced. Depletion of material from patches was assessed by monitoring bed load during the following 5-minute period (hereafter *Pdep*). After the second period the net was removed, emptied again and the flume was then moved to another location. In the laboratory, bed load samples were dried, sieved, weighed and truncated to 1 mm, in order to obtain bed load transport rates and GSDs. Bed load sorting coefficient ($\sigma_{F\&W}$) was calculated for each sample using the index proposed by *Folk and Ward* [1957].

[21] Patches in the study reach are surrounded by larger clasts and typically contain some larger particles mixed within the fine material (Figure 2b). Depending on patch dimensions and the sizes of the larger particles relative to fine patch material, hiding effects created by large grains influence the entrainment of patch sediments. To illustrate a range of possible hiding effects, two extreme values of hiding were calculated and used to correct estimates of critical shear stress derived using the Shield's equation. Hiding was quantified using the function ε, as given by *White and Day* [1982]:

$$\varepsilon_i = \left[0.4(D_i/D_u)^{-0.5} + 0.6\right]$$

where ε_i is the hiding function of a particle of size i, D_i is the size i (m) of a particle, and D_u is a representative surface grain size. The hiding function is normally used in entrainment equations to account for sheltering and high pivot angles of small grains between the interstices of a coarse grained bed. Although the scales are different, a similar principle can be applied to the sheltering effect of large clasts surrounding patches of fine material. Hiding was calculated using two different D_u values: (1) using the GSD for the whole reach to derive the representative surface grain size (i.e., $D_u = 1.6D_{50\text{-}s}\,(D_{84\text{-}s}/D_{16\text{-}s})^{-0.28}$, as per *White and Day* [1982]), and (2) using the average median sized material found in patches as the representative surface grain size (here, $D_u = D_{50\text{-}p}$).

[22] Hiding functions (ε) were then used to define the limits of possible corrections to the theoretical critical shear stress. Depending on their value, corrections either reduce or increase the critical shear stress and give what is called the effective shear stress [*Sutherland*, 1992]. Critical shear stress was calculated using the *Shield*'s [1936] equation:

$$\tau_{c-Di} = \tau_c^* D_{50-pn} \rho' g$$

where $\tau_{c\text{-}Di}$ is the theoretical critical shear stress (N/m^2) for a particle size $D_{50\text{-}pn}$, ρ' is the submerged sediment density (kg/m^3), $D_{50\text{-}pn}$ is the median particle diameter (m) of the patch n (four types of patches; Figure 2a), g is the acceleration to gravity (m/s^2) and τ_c^* is the dimensionless shear stress or Shield's number modified for gravel mixtures (0.045; e.g., *Church* [2006]). The effective shear stress is then calculated as $\varepsilon_i\ \tau_{c\text{-}Di}$.

4. Results

4.1. Hydraulics and Bed Load

[23] Shear stress and associated bed load rates for all experimental locations are shown in Table 2. Water depth inside the flume varied from patch to patch, with a minimum of 0.09 and a maximum of 0.41 m. Mean velocity (i.e., $0.4 \times d$) ranged from 0.20 to 2.14 m/s^1.

[24] Local τ_b during the first 5-minute period of the manipulation (*Pent*) ranged from 0.2 to 40.6 N/m^2, with a mean of 10.3 N/m^2 (σ = 9.9). Local τ_b during the second period (*Pdep*) ranged from 0.2 to 25.6 N/m^2 mean = 8.1 N/m^2, σ = 6.4). Most of the shear stress values in the *Pdep* experiments were identical or very similar to respective *Pent* ones (Table 2), as would be expected given that there was no difference in the level of manipulation. The difference between the maximum shear stress recorded in *Pent* and *Pdep* experiments can be attributed almost exclusively to sample location 21 where calculated shear dropped between the two sampling periods (Table 2).

[25] No bed load was recorded outside the flume during the experimental period (i.e., none of the nets placed upstream of the flume contained sediment [*Gibbins et al.*, 2007b]). Bed load transport occurred at 23 of the 30 locations during the *Pent* sampling period (Table 2). At these locations, bed load transport (i_b) ranged from 0.002 to 5.2 g/sm (mean 0.98 g/sm, σ = 1.6), with 74% of rates being less than 1 g/sm. Median material ($D_{50\text{-}bl}$) in *Pent* samples varied between 1.4 and 2.5 mm (mean $D_{50\text{-}bl}$ was 1.7 mm and σ was 0.3). Two of the twenty three samples had a $D_{50\text{-}bl}$ in the range of gravels while almost all median sizes fell within the coarse sand fraction (Figure 4a) and were in the range of the average median material in the patches (Figure 2a). The largest particles ($D_{max\text{-}bl}$) in *Pent* samples ranged from 3 to 41 mm. Mean $D_{max\text{-}bl}$ was 10.8 mm (σ = 10.9). Sorting coefficient for the *Pent* samples ($\sigma_{F\&W}$) ranged from very well to poorly sorted, while mean $\sigma_{F\&W}$ was 0.66 (moderately well sorted; Table 2). Figure 4a shows the bed load GSDs of all the samples obtained during *Pent* experiments.

[26] During the *Pdep* experiments, mean bed load was an order of magnitude lower than in *Pent* experiments (mean 0.12 g/sm, σ = 0.13; Table 2). Bed load was recorded in 12 of the 30 *Pdep* experiments, with rates varying from 0.002 to 0.330 g/sm. Mean $D_{50\text{-}bl}$ was 1.62 mm (σ = 0.1), almost the same as calculated for the *Pent* samples. The median size of bed load material in this second 5-minute period varied from 1.2 and 1.6 mm, a lower range than in the first period. None of the *Pdep* bed load largest sizes fell within the coarse gravel range (Figure 4b), while the mean maximum size was 5.6 mm (σ = 3.3), almost half that of the *Pent* experiments. Sorting coefficients of the *Pdep* bed load samples indicated very well to moderately sorted material; the mean sorting coefficient of the *Pdep* sample data was 0.61, indicating moderately well sorted bed load in the second 5-minute period of flow manipulation (Table 2). Figure 4b shows the bed load GSDs of all the samples obtained during *Pdep* experiments.

4.2. Entrainment of Patch Material

[27] The relation between shear stress and bed load rates for the *Pent* samples is shown in Figure 4c. Bed load was observed in 43% of the experiments where shear stress was lower than 2 N/m^2 and in 75% of the experiments where shear stress was between 2 and 10 N/m^2. Bed load was recorded in all *Pent* experiments in which shear stress was greater than 10 N/m^2 (Figure 4c and Table 2).

[28] The Shield's equation yielded critical shear stresses for patch sediments of between 0.41 N/m^2 (finest patch, i.e.,

Table 2. Boundary Shear Stress and Bed Load Characteristics During the Flume Experiments

	Experiments									
	Pent[a]					*Pdep*[a]				
Location	τ_b[b] (N/m^2)	i_b[c] (g/sm)	$D_{50\text{-}bl}$[d] (mm)	$D_{\max\text{-}bl}$[e] (mm)	σ_{bl}[f]	τ_b[b] (N/m^2)	i_b[c] (g/sm)	$D_{50\text{-}bl}$[d] (mm)	$D_{\max\text{-}bl}$[e] (mm)	σ_{bl}[f]
1	1.8	0.0758	1.48	4	0.42	1.8	0.0178	1.5	4.0	0.50
2	7.4	–[g]	–	–	–	7.4	0.0035	1.4	1.5	0.31
3	3.9	0.0121	1.49	3	0.44	3.9	0.0020	1.6	3	0.55
4	6.6	–	–	–	–	6.6	–[g]	–	–	
5	11.2	0.2388	1.56	5	0.57	8.3	–	–	–	–
6	10.8	0.0778	1.51	4	0.45	10.8	–	–	–	–
7	9.1	0.0236	1.49	3	0.43	9.1	–	–	–	–
8	8.9	0.0053	–[h]	–	–	8.9	–	–	–	–
9	6.2	0.0017	–	–	–	6.2	–	–	–	–
10	1.0	0.0057	1.51	3	0.45	1.0	–	–	–	–
11	7.9	0.0086	1.62	3	0.46	7.9	–	–	–	–
12	0.2	–	–	–	–	0.2	–	–	–	–
13	1.1	–	–	–	–	1.1	–	–	–	–
14	13.0	0.0173	2.52	6	0.96	13.0	–	–	–	–
15	7.4	0.0035	–[i]	–[i]	–[i]	7.4	–	–	–	–
16	9.3	0.4561	1.54	12	0.54	8.3	0.0265	1.4	3.0	0.62
17	18.2	0.4133	1.53	5	0.50	7.4	0.3073	1.6	8.0	0.59
18	12.8	0.2058	1.63	5	0.61	9.6	0.0091	1.7	3.0	0.59
19	25.0	1.4595	1.73	12	0.83	22.0	0.3301	1.8	13.0	0.79
20	19.6	3.6592	1.82	26	0.95	11.7	0.1139	1.7	5.0	0.62
21	40.6	3.6617	1.90	41	1.22	18.1	0.2293	1.8	7.0	0.77
22	33.7	5.1775	1.84	32	1.16	25.6	0.2293	1.7	7.0	0.73
23	24.6	4.3046	1.97	16	0.90	18.8	0.1206	1.7	9.0	0.64
24	1.2	–	–	–	–	1.2	–	–	–	–
25	4.6	0.0084	1.66	5	0.62	4.6	–	–	–	–
26	1.8	2.3113	2.08	14	0.79	1.8	–	–	–	–
27	3.6	–	–	–	–	3.6	–	–	–	–
28	3.4	0.3399	1.61	7	0.57	3.4	0.0096	1.6	4.0	0.57
29	1.2	–	–	4		1.2	–	–	–	–
30	12.0	0.0043	1.41	–[i]	0.31	12.0	–	–	–	–
Mean	10.27	0.98	1.70	10.84	0.66	8.17	0.12	1.62	5.63	0.61
Standard deviation	9.9	1.6	0.3	10.9	0.3	6.4	0.13	0.1	3.3	0.1

[a]*Pent*, patch entrainment experiments; *Pdep*, patch depletion experiments (see section 3.2 for further details).
[b]Boundary shear stress [*Whiting and Dietrich*, 1990].
[c]Instantaneous bed load transport rate.
[d]Median bed load particle size.
[e]Maximum bed load particle size.
[f]Bedload sorting index [*Folk and Ward*, 1957].
[g]No finite bed load collected. Note than in the case of location 2, bed load was collected in the *Pdep* experiment, an unusual observation.
[h]Particle size analyses could not be done due to the small size of the sample.
[i]Maximum bed load particle size could not be sampled due to the small size of that.

D_{50} = 0.57 mm) and 1.59 N/m^2 (coarsest patch, i.e., D_{50} = 2.2 mm). Thus theoretically, bed load transport could be expected to occur from patches when shear stress is within the range of 0.4–1.6 N/m^2. However, bed load was recorded from only one (25%) of the *Pent* experiments with shear stress within this range (Table 2).

[29] Table 3 shows hiding functions (ε_i) for fine and coarse patches and effective shear stress values calculated using these functions as multipliers on the critical shear stress values obtained using the Shield's equation (i.e., $\tau_{c\text{-}Di}$). The effective shear stress values calculated using reach scale GSD data for hiding suggest that entrainment should not be expected below 1.8 N/m^2 in fine patches while it could be expected in coarser patches once shear stress exceeds 4 N/m^2. The range of effective shear stress decreases to 0.48–1.28 N/m^2 (fine and coarse patches respectively) when the median patch GSD (i.e., $D_u = D_{50\text{-}p}$) is used for hiding (Table 3). Bed load was recorded in almost all (90%) of *Pent* experiments in which shear stress exceeded 4.1 N/m^2, while it was recorded in only one experiment in which shear stress was less than 1.28 N/m^2. These values suggest that, in the case of the Ribera Salada, hiding is best estimated using GSD data from the reach rather than the patch and that that critical shear stress for entrainment of median particle sizes in the patches should be considered to be between 2 and 5 N/m^2.

4.3. Comparison of Bed Load With Patch Material

[30] Because of the experimental design, it is self evident that the main sources of sediment during the manipulations are the patches. However, the exact degree to which bed load GSD*s* resemble those of the patches is not directly known and so is worthy of analysis.

[31] The mean median bed load particle size of the *Pent* experiments was similar to the mean of the patches (Table 2). Increases in shear stress did not result in increases in the median size of bed load material (Figure 4e). However, maximum particle sizes increased as shear stress increased. These patterns indicate that particles from the patches and

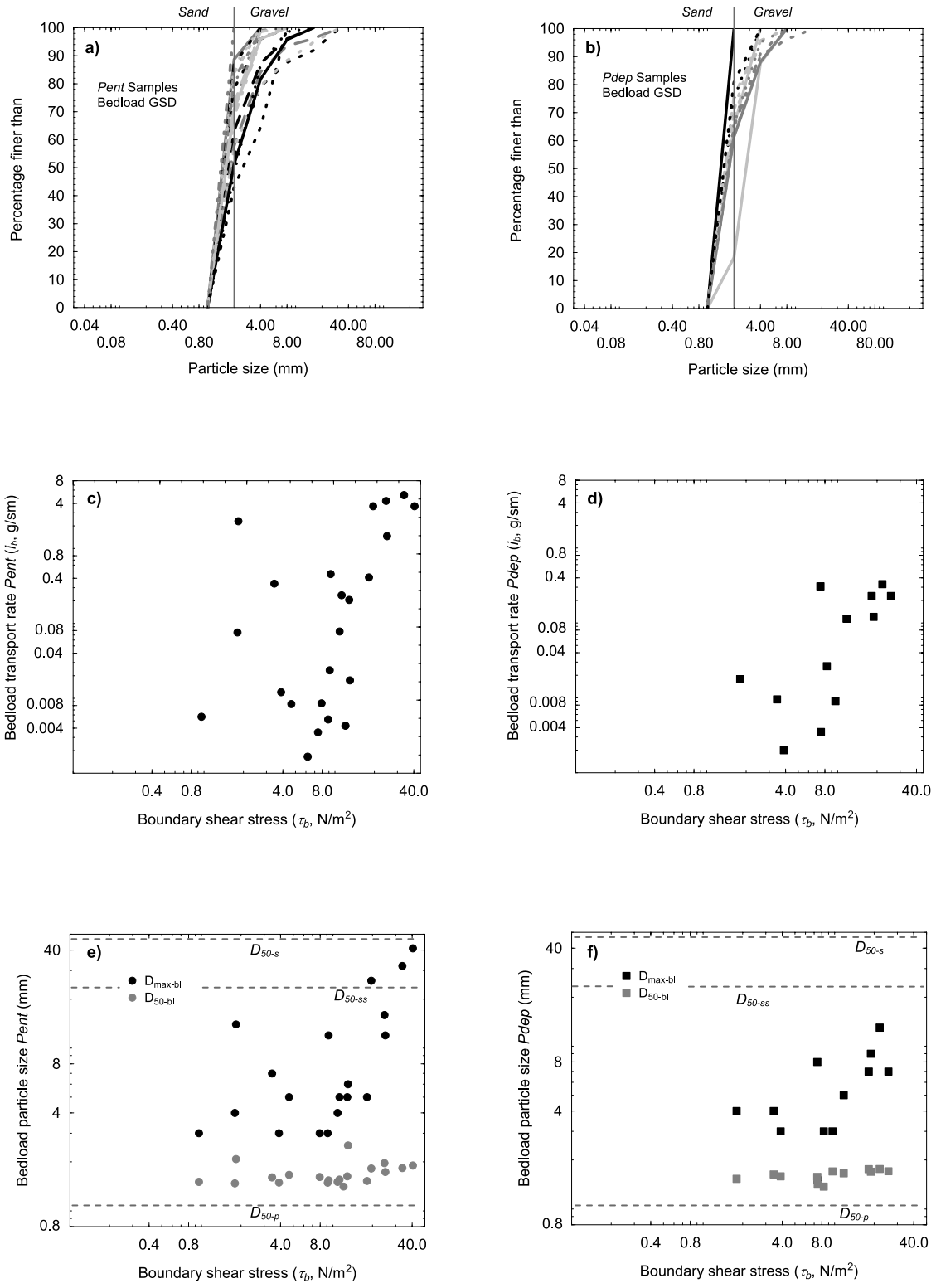

Figure 4. Grain size distributions of (a) Patch entrainment (*Pent*) and (b) depletion (*Pdep*) bed load samples. Relations between shear stress and (1) bed load transport for (c) *Pent* and (d) *Pdep* experiments, and (2) largest and median particle size obtained in the bed load samples during (e) *Pent* and (f) *Pdep* experiments. Note that in c and d zero rates are not plotted and that the median particle sizes of the surface, subsurface and patch sediments are presented for reference in e and f (see Table 2 for raw data).

Table 3. Comparison of Hiding Functions for fine ($D_{50\text{-}p}$ 0.57 mm) and Coarse ($D_{50\text{-}p}$ = 2.2 mm) Patches Derived Using Grain Size Values From the Reach and Patch Scales[a]

Representative Surface Grain Size[b]	Hiding Function (ε)		Effective Shear Stress (N/m^2)	
	Fine Patch	Coarse Patch	Fine Patch	Coarse Patch
	D_{50} = 0.57 mm	D_{50} = 2.2 mm	D_{50} = 0.57 mm	D_{50} = 2.2 mm
Reach average GSD[c]	2.6	4.4	1.8	4.1
Patch average GSD[d]	0.85	1.17	0.48	1.28

[a]Corresponding effective shear stress values (calculated using ε as a multiplier on the critical shear stress estimated using the Shield's equation i.e., $\varepsilon_i\ \tau_{c\text{-}Di}$). See text for discussion.

[b]Hiding was calculated considering two different D_u values:

[c]GSD was used for the whole reach to derive the representative surface grain size (i.e. $D_u = 1.6D_{50\text{-}s}\ (D_{84\text{-}s}/D_{16\text{-}s})^{-0.28}$, as per *White and Day* [1982]).

[d]Average median sized material found in patches was used as the representative surface grain size (i.e., $D_u = D_{50\text{-}p}$).

those in the range of coarse sand ($\sim D_{50\text{-}p}$) do not experience size selective transport while the largest sizes have selective transport across almost the full range of boundary shear stresses created during the *Pent* experiments.

[32] Size selective transport of the material from the patches was quantified using fractional bed load transport rates. Fractional bed load transport rates (i.e., $i_{b\text{-}i}$, where $i_{b\text{-}i} = i_b p_{bl\text{-}i}$, and $p_{bl\text{-}i}$ is the proportion of bed load in fraction i) were scaled by the proportion of each size fraction i in the material from the patches (i.e., $p_{p\text{-}i}$). An average grain size distribution from the four patches presented in Figure 2a was used to calculate $p_{p\text{-}i}$. Scaled fractional bed load transport rates were plotted against the relative size i, calculated by scaling each size (D_i) by the average median patch size ($D_{50\text{-}p}$) [e.g., *Wilcock*, 1992]. Fractional bed load rates were grouped by shear stress intervals: (1) samples between 5 and 10 N/m^2, (2) samples between 10 and 20 N/m^2, and (3) samples where shear exceeded 20 N/m^2. Samples where shear stress was less than 5 N/m^2 were omitted because this is within range of entrainment thresholds estimated for the patches (section 4.2). Figure 5a shows that at shear stress between 5 and 10 N/m^2 scaled fractional bed load rates have a negative linear trend. This trend suggests that bed load transport during these conditions was size selective. When shear stress was between 10 and 20 N/m^2, the fine (coarse sands) and the coarsest (medium gravels) particle sizes were overrepresented in relation to the average patch GSD. Even so the fairly flat and smooth pattern of the trend suggests that mobility for all the sizes during the experiments was not markedly different. During experiments with the highest values of shear stress (>20 N/m^2), fine particles were overrepresented while the largest particles trended to have partial mobility. The mobility of all particle sizes when shear stress was higher than 10 N/m^2 was one order of magnitude higher than when the shear was less than 10 than N/m^2. For shear stresses higher than 20 N/m^2 a peak in mobility was found for a particle sizes of 2 mm (i.e., $D_{i\text{-}bl}/D_{50\text{-}p} = 1.67$). Afterward, mobility decreased and stabilized when $D_{i\text{-}bl}$ reached 8 mm.

[33] These results suggest that bed load transport from patches was strongly selective when the shear stress acting on the patch was close to the critical threshold (5–10 N/m^2). Above 10 N/m^2 bed load transport from patches approached equal mobility. At high shear stresses (>20 N/m^2) the negative slope of the curve after $D_{i\text{-}bl}$ = 8 mm showed a

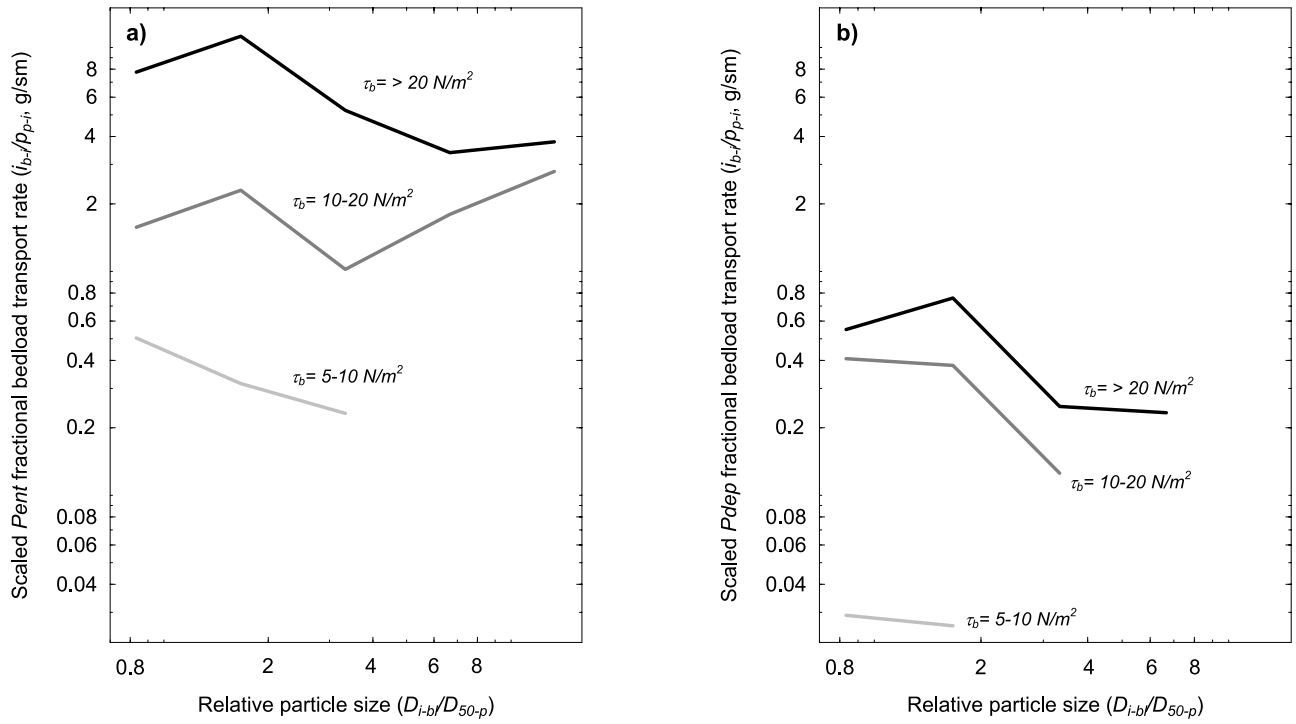

Figure 5. Relation between scaled fractional bed load transport rates (i.e., $i_{b\text{-}i}/p_{p\text{-}i}$) and the relative particle size (i.e., $D_{i\text{-}bl}/D_{50\text{-}p}$) for (a) *Pent* and (b) *Pdep* samples obtained during the experiments. Raw data were grouped by shear intervals.

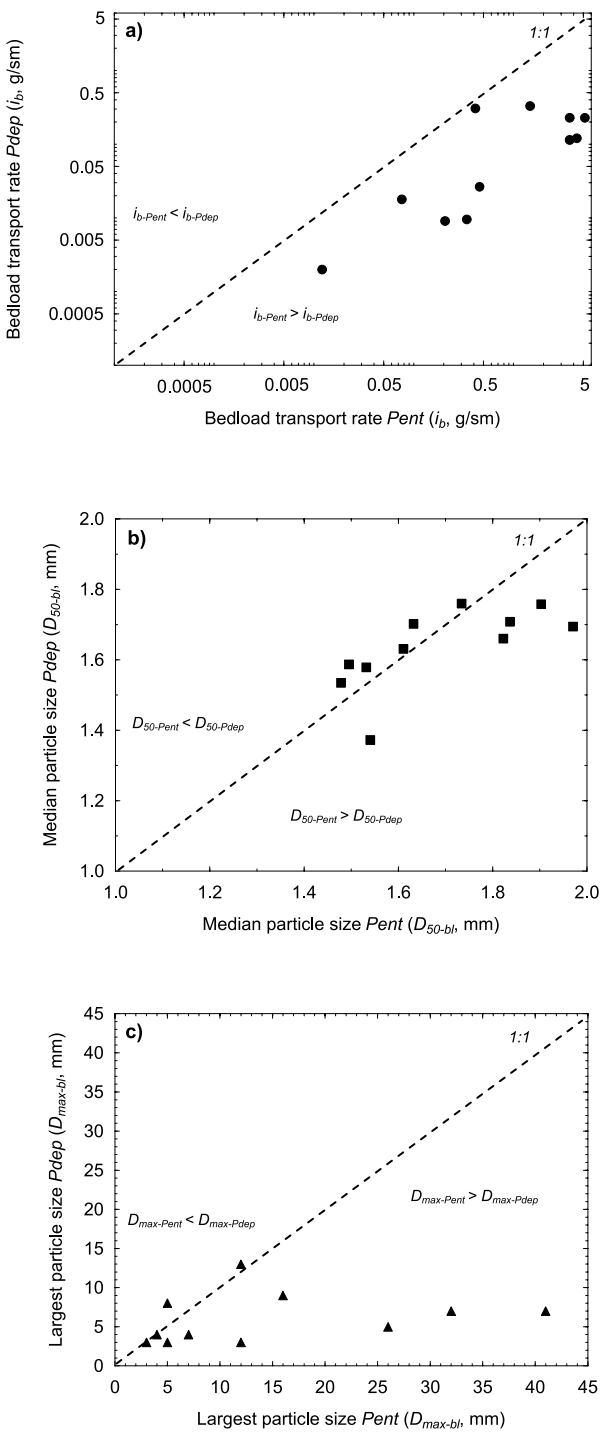

Figure 6. Comparison between entrainment (*Pent*) and depletion (*Pdep*) bed load samples: (a) bed load transport rates, (b) median bed load particle sizes, and (c) largest particle sizes. Note that the 1:1 relation is indicated as a reference.

selective pattern that could be attributed to the depletion of material from the patches.

4.4. Sediment Depletion

[34] During natural flood events, sediment lost from patches should be replaced by material transported from upstream. However, studies have shown that this replacement tends to vary between floods [*Laronne et al.*, 2001]. *Garcia et al.* [1999] reported that during events that lack the competence to entrain the entire river-bed, patches with fine sediments represent the main source of bed load, at least until their area extent is reduced. Thus under certain natural conditions, patches can be depleted without material being replaced from upstream. Data from the *Pdep* experimental periods allow assessment of depletion processes under such conditions.

[35] Twelve of the *Pdep* samples contained bed load (Table 2). The relation between shear stress and bed load rates for these experiments is presented in Figure 4d. Although bed load rates for the *Pdep* experiments increased with increasing shear stress, the maximum rates are one order of magnitude lower than the obtained for the *Pent* experiments with similar shear stress (Figure 4c and Table 2). As with the *Pent* experimental data, $D_{50\text{-}bl}$ in the P*dep* experiments did not change with increasing shear stress, while the size of the $D_{\max\text{-}bl}$ increased as shear increased (Figure 4f). Figure 6a compares i_b for the *Pent* and *Pdep* experiments and shows that bed load rates decreased substantially after 5 minutes. These patterns indicate depletion of source material.

[36] Median and maximum particles sizes collected in the two phases of the experiments are compared in Figures 6b and 6c, respectively. Median bed load particles during the *Pent* experiments were almost the same (5% of difference) as those obtained for the *Pdep* experiments, while the largest particles were clearly (48%) larger. These differences are related to the depletion process itself. Size fractions smaller than and around the mean size of material present in the patches were the most overrepresented ones in the *Pent* bed load (Figure 5a). Data therefore suggest that these size fractions were flushed in mass in the first 5 minutes of the flow manipulation, with their availability during the second 5 minutes limited by this loss. Only some of the larger particles remained available for transport in the second 5-minute period. However, the absolute number of particles around the size of the largest particle found in the *Pent* samples was relatively small. Consequently, in circumstances in which sediments in the patches were still available, median bed load particle sizes in the *Pdep* experiments become coarser than in the *Pent* phase, while the largest particle transported tended to be smaller because of the prior depletion.

[37] Fractional bed load transport rates during *Pdep* experiments are presented in Figure 5b. All the trends have a negative slope, indicating that fractions between fine and medium gravels were less well represented than coarse sand particles. Across the whole range of shear stress values, the mobility of all particle sizes was almost one order of magnitude lower than observed in the first 5-minute period (Figure 5a). These results suggest that depletion occurred after only 5 minutes, with bed load transport strongly size selective at all shear stresses created by the manipulations. Under such conditions, bed load transport is more controlled by the availability of sediment in the patches than by the hydraulic forces acting on them.

4.5. From Incipient to Near-Full Transport: Combining Evidence From Experiments and Measurements

[38] Figure 7 shows changes in bed load transport rates at shear stresses ranging from 5 to almost 60 N/m^2. The data

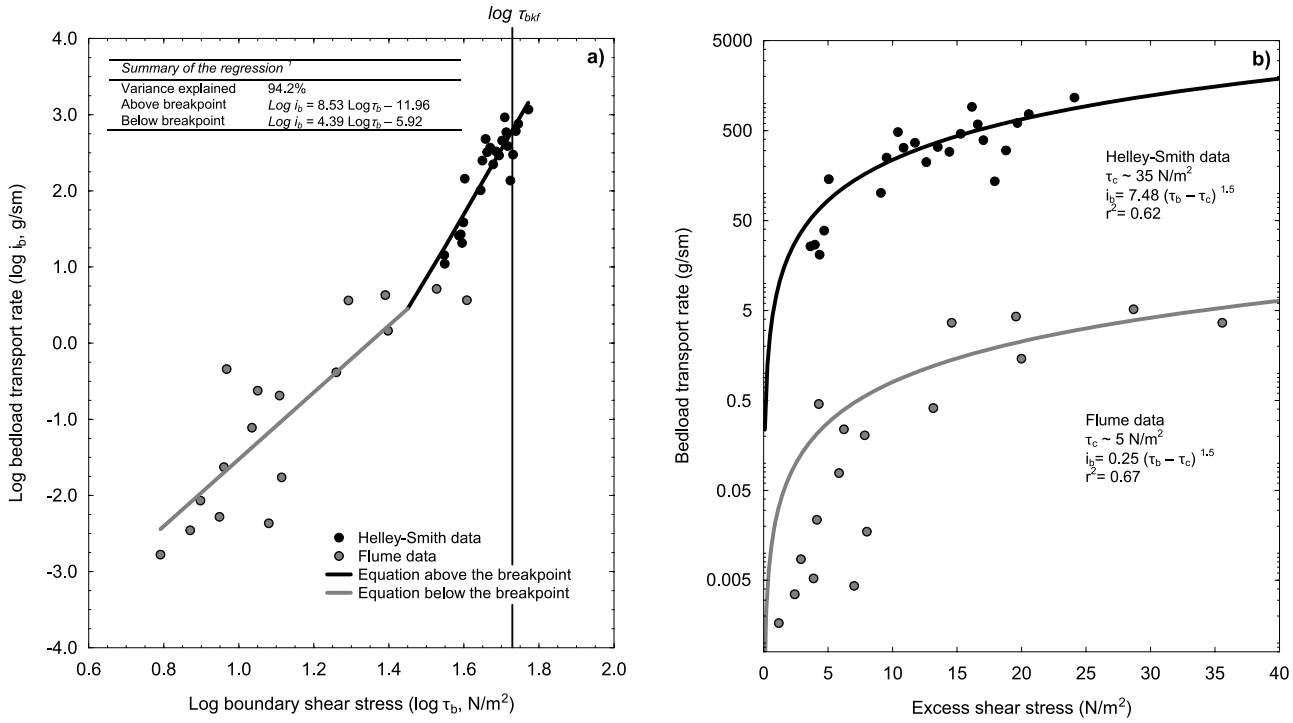

Figure 7. (a) Log-log relation between bed load transport rates and shear stress combining the flume data obtained during the experiments and the data collected with a 76-mm intake Helley-Smith (HS76) sampler during a series of floods (see *Batalla et al.* [2005] for more details). A piecewise linear regression was fitted to the log-log data (details of the regression are included in the figure). Note that the log shear stress attained during bankfull discharge is indicated (log τ_{bkf}). (b) Relation between bed load transport rates and excess shear stress ($\tau_b - \tau_c$) both for the flume data obtained during the experiments and the data collected during floods. Critical shear stress (τ_c) for the flume experiments has been considered at 5 N/m^2 while for the data obtained during the experiments this value has been estimated at 35 N/m^2 (after *Batalla et al.* [2005], see discussion in the text).

set has been compiled by combining the flume bed load data (Table 2) with that collected using a 76 mm intake Helley-Smith sampler (hereafter HS76) during a series of floods [*Batalla et al.*, 2005] in a cross section located in the middle of the study reach. A shear stress of 5 N/m^2 has been taken as the critical threshold for patch entrainment (discussed in section 4.2), so flume bed load data obtained for shear stresses <5 N/m^2 have been omitted. Helley-Smith samples were obtained at different verticals (following regular step distances) across the section. Bed load rates shown in Figure 7 represent the mean of the samples collected across the section (see *Batalla et al.* [2005] for more details). Piecewise linear regression was used to define statistical relations between shear stress and bed load transport rates for flume and HS76 data (see inset in Figure 7a). Following *Ryan et al.* [2002], the point where the linear regressions intersect is termed the breakpoint.

[39] Below the breakpoint the line represents the sand mobility phase and the initiation of gravel entrainment (i.e., size-selective transport). Only a small number of flume samples fall above the breakpoint, while all the HS76 samples sit above it. The highest flume and the lowest HS76 values occur around the breakpoint (centered at approximately 30 N/m^2, 1.47 in log units). Consequently, flume and HS76 bed load data converge, suggesting that there is no marked difference in sampling efficiency at this shear stress.

[40] Differences in bed load characteristics between the samples that define the two regression lines can be seen by comparing GSDs. Mean $D_{50\text{-}bl}$ of the samples collected by the HS76 ($D_{50\text{-}bl}$ = 3.3 mm) was coarser than that from the *Pent* flume experiments ($D_{50\text{-}bl}$ = 1.7 mm). Importantly, these median values do not differ markedly from the median particle sizes in the patches (Figure 2a). A similar pattern is found in the case of the larger particle sizes in the GSDs (e.g. HS76 $D_{95\text{-}bl}$ = 15 mm; *Pent* $D_{95\text{-}bl}$ = 6.1 mm). Even the largest sizes collected by the HS76 were much smaller than the overall $D_{50\text{-}s}$ of the study reach. This may be related to the performance of the HS76 sampler in such an environment [*Vericat et al.*, 2006] and/or to the fact that full mobility had not been reached across the reach.

[41] Bed load was less sorted (mean $\sigma_{F\&W}$ = 1.6, grain size is less uniform) in the samples above the breakpoint, indicating that during natural flood events bed load is not just controlled by river-bed dynamics at the patch scale. When the coarse surface layer starts to shake, subsurface material enhances sediment availability and so transport variability increases. The sorting was much higher in the data derived from the flume experiments (mean $\sigma_{F\&W}$ = 0.66). This could be biased because bed load samples were truncated at 1 mm (see methods for more details), or it could

reflect the fact that bed load during flume experiments was controlled only by the local sediment sources (i.e., patches) which are homogeneous relative to the reach overall.

[42] Figure 7b shows the relation between excess shear stress and bed load transport rate for flume and HS76 data. Excess shear stress was calculated as the difference between boundary shear stress (τ_b) and the critical shear stress (τ_c) for respective data sets. In the case of the flume experiments, 5 N/m^2 (section 4.2) was taken as the critical shear stress while for the HS76 data a value of 35 N/m^2 was used [as per *Batalla et al.*, 2005]. Thus critical shear stresses are empirically derived rather than being calculated theoretically using the Shield's equation. A *Meyer-Peter and Müller* [1948] style equation $i_b = a\ (\tau_b - \tau_c)^b$ was fitted to each shear stress-bed load relation (where a is a coefficient and b is a constant value at 1.5; details in Figure 7b). The relations in Figure 7b have a convex inflection, indicating a rapid increment of i_b as soon threshold stress is reached. The relative increment of i_b tends to decrease when the excess shear stress is higher than 10 N/m^2. The equation fitted for the flume experiments has a lower a constant value than that of the HS76 data. Moreover, bed load rates predicted by the equations differ by more than two orders of magnitude for the same excess shear stress. This difference is related to the limited availability of sediment in the patches: in the flume data, above the threshold, bed load is controlled only by the patches whereas when sampling is conduced at reach scale (i.e., sampling in a cross section, as in the case of the HS76 data), the potential source of sediment is the entire upstream channel, including surface particles, patch materials and even subsurface sediments. Equations presented in Figure 7b represent bed load *Phases I* and *II* models in the study reach.

5. Discussion and Conclusions

[43] This study provides further support for the argument that sediment entrainment and hence bed load transport rates depend critically on bed sediment structures. Poorly sorted gravel bed rivers often have armored bed surfaces that remain stable under a wide range of flow conditions. However, areas of exposed subsurface material or patches of fine sediment [*Laronne et al.*, 2001; *Brayshaw et al.*, 1983] that are normally protected by large coarse clasts may be mobilized by frequent, small to medium sized floods. Based on the flow frequency analysis reported by *Batalla et al.* [2005], *Gibbins et al.* [2007b] estimated that the hydraulic conditions created by the flume manipulations in the Ribera Salada study reach are those typically associated with small floods and/or the early stages of larger flood events. Thus patches of fine material may be the principal source of sediment in low bed load conditions associated either with small, frequent events or transient periods of low bed load transport that occur in the early stages of larger floods [*Garcia et al.*, 1999]. However, the limited size of patches dictates that their contribution will be time-limited, since at some point depletion will occur.

[44] Although low magnitude floods have limited impact on reach scale geomorphology, even low rates of bed load transport can have marked ecological effects [*Gibbins et al.*, 2007a, 2007b]. Thus understanding the processes and controls on entrainment during low bed load conditions has importance beyond fluvial geomorphology. Historically, technical difficulties have prevented a clear understanding of entrainment in natural channels during small flood/low bed load conditions. Along with that of *Garcia et al.* [2007], the present study provides rare and novel field data that describe entrainment processes in patches of fine material. Cross-sectional average critical shear stress is often used as the threshold to define the transition between bed stability and instability. However, it is widely acknowledged that some bed load transport may occur below this critical value. A clear example is the HS76 bed load data obtained in the Ribera Salada study reach by *Batalla et al.* [2005]: although theoretical average critical shear stress was found at around 40 N/m^2, bed load samples were obtained at shear stresses of 35 N/m^2. Flume experiments have provided the opportunity to observe and quantify bed load transport in the same reach at much lower shear stresses. It has been hypothesized that this marginal bed load transport can be attributed to the mobilization of grains from patches of fine material. Our study provides the first empirical evidence that can be used to test this hypothesis. Overall, by marrying the experimentally derived flume data with information collected at higher shear stresses using a Helley-Smith sampler, we have been able to assess bed load transport at shear stresses ranging from 5 to 60 N/m^2.

[45] The flume bed load transport rates were very low, with even the maximum (<6 g/sm) equating only to partial bed load transport [as defined *Wilcock and McArdell*, 1993; *Church and Hassan*, 2005]. *Church and Hassan* [2005] reported similarly low rates of bed load transport in Harris Creek, a cobble-gravel stream in British Columbia. These authors simulated field conditions in a laboratory flume in order to examine the hydraulic role of bed structures. They reported a threshold for sand movement of around 4 N/m^2 while the onset of gravel transport was calculated to be at around 15 N/m^2. For the mean conditions of the experiments they calculated a dimensionless critical shear stress value (τ_c^*) of 0.079. Our in-stream flume experiments in the Ribera Salada yielded a τ_c^* value between 0.073 (based on the lower critical shear stress value reported in section 4.2 and the mean $D_{50\text{-}ib}$) and 0.182 (based on the larger critical shear stress value reported in section 4.2). This range does not differ substantially from that reported by *Church and Hassan* [2005] but is clearly higher than the classical Shield's datum. Bed load occurred in all the patch entrainment experiments (first 5-minute period of hydraulic manipulation) when shear stress was greater than 10 N/m^2. When shear stress was less than 2 N/m^2 bed load was observed in only 43% of cases (Figure 4c and Table 2). As has been described in other gravel bed rives, results for the Ribera Salada indicate that the hiding effect is most likely responsible for the absence of sediment transport under conditions above the theoretical shear stress (calculated using the Shields equation) for patch entrainment.

[46] The data on fractional bed load transport rates obtained from the experiments show that transport from patches is strongly selective when the shear stress is in the range of the entrainment threshold (5–10 N/m^2). This has been found in rivers with bimodal sediments [e.g., *Wathen et al.*, 1995]. When shear stress increases beyond the threshold, bed load transport from patches approaches equal mobility (i.e., general sand transport). In the Ribera Salada, patch depletion controls the availability of sediments at

shear stresses >20 N/m^2 and, consequently, equal mobility of patch sediments no longer occurs.

[47] In the early stages of floods, material from patches is mobilized and comprises the main source of bed load in gravel bed rivers. At this stage partial bed load occurs at the reach scale. Although this condition may be frequent and may have marked ecological effects [*Gibbins et al.*, 2007b], observations of partial bed load transport in the field are difficult because of the spatial variability in bed topography and composition. This variability makes it difficult to properly assess the spatial extent and local variability of grain entrainment [*Haschenburger and Wilcock*, 2003]. We have demonstrated that the portable flume can overcome this limitation and can help provide quantitative data on partial bed load transport at patch scale.

[48] As shear stress increases further, coarse material is progressively entrained, the armor starts breaking up and, at some point, surface and subsurface material across the entire bed contributes to bed load transport. The breakup of the armor layer increases both sediment availability and bed load variability (rates and size range). Thus several inflections in the relation between shear stress and bed load transport can be expected. By combining bed load data from flume experiments and a Helley-Smith sampler, we have identified the first of the breakpoints in this relation. Although bed load samples collected with the HS76 may be affected by blockage and "perching" [*Vericat et al.*, 2006] it is clear from Figure 7 that the two groups of samples converge. This convergence suggests that there is no marked difference in the efficiency of two methods when they are operating at the same shear stress. In turn, this suggests that flume and HS76 data can be integrated to help identify inflections or breakpoints in bed load transport rates. In the Ribera Salada study reach, a breakpoint occurred at a shear stress around 30 N/m^2 (equating to an instantaneous discharge of 2.3 m^3/s). This is almost coincident with the theoretical critical threshold to entrain the median surface particle size of the reach ($\sim$35 N/m^2).

[49] The shift between bed load transport *Phases I* and *II* of *Jackson and Beschta* [1982] has been documented to occur near bankfull discharge, when fully mobile conditions are reached [*Parker et al.*, 1982; *Andrews*, 1984; *Andrews and Nankervis*, 1995]. *Ryan et al.* [2002] compared discharge at the phase shift to bankfull discharge in twelve gravel bed channels in Colorado and Wyoming (USA). They found that a shift between phases typically occurred at about 80% of bankfull discharge. In a river with similar hydrologic and geomorphic conditions to the Ribera Salada, *Haschenburger and Wilcock* [2003] observed fully mobile conditions during a flood that approximately equaled the bankfull discharge. The breakpoint in the Ribera Salada data set occurred at only 23% of the bankfull discharge ($\sim$2.3 m^3/s), while field observations in the study reach have shown that bankfull conditions (τ_{bkf} = 54 N/m^2) are required for full mobility to occur [*Batalla et al.*, 2005]. Thus we conclude that the breakpoint in the Ribera Salada does not define the transition between *Phases I* and *II* of *Jackson and Beschta* [1982].

[50] *Ashworth and Ferguson* [1989] proposed a three phase model of bed load transport. The Ribera Salada data below the breakpoint correspond to their *Phase I*. In gravel bed rivers such as the Ribera Salada, patches are the main source of bed load during this phase; for example, between 50 and 90% of the bed load particle sizes fit between the coarse sand and fine gravel classes that are typical of patches. At a reach scale, this phase may be described as partial transport because surface grains remain largely immobile [*Wilcock and McArdell*, 1993, 1997]. At a patch scale, however, almost all material is entrained and fully mobile conditions are reached. As shear stress increases and approaches the first breakpoint in the three phase model, medium to coarse gravels in patches start to entrain, the coarse surface layer becomes unstable, at least locally, transport rates increase and bed load material coarsens. This is *Phase II* of *Ashworth and Ferguson* [1989]. When shear stress increases some parts of the channel may shift from partial to fully mobile conditions (see *Haschenburger and Wilcock* [2003] for a complete map of partial and fully mobile areas under different shear stresses). Full bed mobility conditions in the Ribera Salada study reach are expected when shear stress approaches that associated with bankfull discharge. Only four HS76 measurements were obtained at bankfull conditions. Thus the lack of observations beyond this value limits the search of a second breakpoint in our data that would indicate a transition between *Phases II* and *III* of the *Ashworth and Ferguson* [1989] classification.

[51] Sampling problems have prevented so far clear insights into low bed load conditions and associated hydraulic controls in natural river channels. The portable flume used in this study has the potential to offer such insights. It permits controlled flow manipulation in natural river channels, free from many of the constraints, which affect laboratory flume studies. Although the design of the flume can be improved upon (see discussion in *Gibbins et al.* [2007b]), it can be used to address questions related to incipient bed load transport, questions beyond the reach of conventional approaches such as Helley-Smith sampling or pit traps. A number of conclusions can be drawn from combined flume and Helley-Smith bed load sample data obtained in the gravel bed experimental reach of the Ribera Salada:

[52] 1. In our analysis, patches of fine sediment exerted a primarily control on bed load transport under hydraulic conditions characteristic of small floods and/or associated with the early stages of large floods.

[53] 2. The flume experiments provided an opportunity to observe and quantify bed load transport at much lower shear stresses than the critical value predicted by the classical Shields equation. Our field study provides the first empirical evidence that this marginal bed load transport can be attributed to the localized mobilization of grains from micropatches.

[54] 3. Patch sediment entrainment depends critically on bed sediment structures. In particular, the hiding effect created by large clasts appears to be responsible for the absence of bed load transport under conditions in which the Shields equation predicts entrainment of the median particle sizes from patches.

[55] 4. Flume data indicate that bed load transport from patches is strongly selective when shear stress is in the range of the critical threshold for patch material. When shear stress increases above this threshold, equal mobility of material in patches occurs.

[56] 5. Depletion of patch material controls the temporal availability of sediments during floods. In the flume experiments, depletion (indicated by changes in bed load rates and size characteristics) was evident after only 5 minutes of flow manipulation.

[57] 6. Sediment loss from patches at low shear stresses is predominantly of fine material (sand) at a low rate (i.e., *Phase I* as per *Ashworth and Ferguson* [1989] and during the final phase in the process of patch entrainment observed by *Garcia et al.* [2007]). Much higher rates of transport occur once shear stress exceeds ~30 N/m^2 (i.e., *Phase II*, as per *Ashworth and Ferguson* [1989]). This threshold corresponds approximately to a discharge of one-fourth of the bankfull, a discharge that in the Ribera Salada is exceeded around 15% of the time. Thus we conclude that changes from *Phase I* to *Phase II* occur regularly in the river.

Notation

- σ Standard deviation
- A_r Armoring ratio; defined as the quotient between the median surface material particle size and the median subsurface material particle size (dimensionless)
- d Water depth (in m)
- $D_{50\text{-}p}$ Median material particle size in patch structures (in mm)
- $D_{50\text{-}pn}$ Median particle diameter of the patch n (in m)
- $D_{50\text{-}s}$ Median surface material particle size (in mm)
- $D_{50\text{-}ss}$ Median subsurface material particle size (in mm)
- D_i Particle of a size i (represented in m or mm in relation to the purpose of the number)
- $D_{i\text{-}bl}$ Percentile i of a bed load grain size distribution (in mm)
- $D_{\max\text{-}bl}$ Largest particle collected on bed load samples (in mm)
- $D_{u\text{-}a}$ Representative surface particle size following *White and Day* [1982] formulation, $D_{u\text{-}a} = 1.6D_{50\text{-}s}\ (D_{84\text{-}s}/D_{16\text{-}s})^{-0.28}$, where $D_{16\text{-}s}$, $D_{50\text{-}s}$ and $D_{84\text{-}s}$ are the respective percentiles in the surface GSD (in m)
- $D_{u\text{-}b}$ Representative surface particle size considering the average median patch size as the representative $D_{u\text{-}b} = D_{50\text{-}p}$
- g Acceleration due to gravity (in m/s^2)
- GSD Grain Size Distribution
- HS76 76-mm intake Helley-Smith sampler
- i_b Bed load transport rate (in g/sm)
- $i_{b\text{-}i}$ Fractional bed load transport rate (in g/sm)
- $i_{b\text{-}m}$ Mean bed load transport rate (in g/sm)
- k Von Karman's constant (equal to 0.40),
- $p_{bl\text{-}i}$ Proportion of bed load in fraction i
- *Pent* Patch entrainment experiments
- *Pdep* Patch depletion experiments
- $p_{p\text{-}i}$ Proportion of a size fraction i in the material from the patches
- v Flow velocity (in m/s)
- v_z Flow velocity at height z above bed,
- ρ' Submerged sediment density (1650 kg/m^3)
- ε Hiding function (calculated in this study following *White and Day* [1982] equation)
- ε_i Hiding function of a particle D_i
- ϕ Phi units ($\phi_i = -\log_2 D_i$, where ϕ_i is the size in phi units of unit of length D_i expressed in mm)
- ρ Water density (1000 kg/m^3)
- $\sigma_{F\&W}$ Sorting coefficient (dimensionless); calculated using the index proposed by *Folk and Ward* [1957]
- τ_c^* Dimensionless shear stress or Shield's number modified for gavel mixtures (0.045)
- τ_b Boundary shear stress (in N/m^2); boundary shear stress was calculated using the formula and criteria proposed by *Whiting and Dietrich* [1990] (see text for more details)
- τ_{bkf} Mean shear stress under bankfull conditions (in N/m^2)
- $\tau_{b\text{-}m}$ Mean boundary shear stress (in N/m^2)
- $\tau_{c\text{-}D50pn}$ Theoretical critical shear stress for a particle size $D_{50\text{-}pn}$ (in N/m^2)
- τ_{cr} Entrainment threshold, critical shear stress (in N/m^2)

[58] **Acknowledgments.** We gratefully acknowledge the Leverhulme Trust for funding the work described in this paper. Damia Vericat was employed on this project with grants from the Catalan Foundation for Research and Innovation and the Leverhulme Trust. We thank Dubrovka Pokrajac and Lorna Campbell for suggestions that helped improve the design of the flume and Robert Ferguson, Ian Reid, Celso Garcia, and Ellen Wohl for the thorough revision of the manuscript.

References

Andrews, E. D. (1984), Bed-material entrainment and hydraulic geometry of gravel bed rivers in Colorado, *Geol. Soc. Am. Bull.*, *95*, 371–378.

Andrews, E. D., and J. M. Nankervis (1995), Effective discharge and the design of channel maintenance flows for gravel bed rivers, in *Natural and Anthropogenic Influences in Fluvial Geomorphology: The Wolman Volume*, edited by J. E. Costa et al., pp. 151–164, *Geophys. Monogr. 89*, AGU, Washington, D. C.

Ashworth, P. J., and R. I. Ferguson (1989), Size-selective entrainment of bed load in gravel bed streams, *Water Resour. Res.*, *25*(4), 627–634.

Batalla, R. J., C. Garcia, and J. C. Balasch (2005), Total sediment load in a Mediterranean mountainous catchment (the Ribera Salada River, Catalan Pre-Pyrenees, NE Spain), *Z. Geomorphol.*, *49*(4), 495–514.

Brayshaw, A. C., L. E. Frostick, and I. Reid (1983), The hydrodynamics of particle clusters and sediment entrainment in coarse alluvial channels, *Sedimentology*, *30*, 137–143.

Bunte, K., and S. R. Abt (2001), Sampling surface and subsurface particle-size distributions in wadable gravel- and cobble-bed streasm for analyses in sediment transport, hydraulics, and streambed monitoring, *Gen. Tech. Rep. RMRS-GTR-74*, 428 pp., U.S. Dept. of Agric., Forest Serv., Rocky Mountain Research Station, Fort Collins, Colo.

Carling, P. A. (1988), The concept of dominant discharge applied to two gravel-bed streasm in relation to channel stability thresholds, *Earth Surf. Process. Landforms*, *13*, 355–367.

Church, M. (2006), Bed material transport and the morphology of alluvial river channels, *Annu. Rev. Earth Planet. Sci.*, *34*, 325–354.

Church, M., and M. Hassan (2005), Upland gravel-bed rivers with low sediment transport, in *Catchment Dynamics and River Processes. Mediterranean and Other Climate Regions*, edited by C. Garcia and R. J. Batalla, pp. 141–168, Elsevier, Amsterdam.

Church, M., D. G. McLean, and J. F. Wolcott (1987), River bed gravels: Sampling and analysis, in *Sediment Transport in Gravel Bed Rivers*, edited by C. R. Thorne, J. C. Barthurst, and R. D. Hey, pp. 43–88, John Wiley, Chichester, U.K.

Egiazaroff, I. A. (1965), Calculation of non-uniform sediment concentrations, *J. Hydraul. Div. Am. Soc. Civ. Eng.*, *91*(HY4), 225–247.

Folk, R. L., and C. Ward (1957), Brazos River bar: A study in the significance of grain size parameters, *J. Sediment. Petrol.*, *27*(1), 3–26.

Garcia, C., J. B. Laronne, and M. Sala (1999), Variable sources of bedload in a gravel-bed stream, *J. Sediment. Res.*, *69*(1), 27–31.

Garcia, C., H. Cohen, I. Reid, A. Rovira, X. Ubeda, and J. B. Laronne (2007), Processes of initiation of motion leading to bedload transport in gravel-bed rivers, *Geophys. Res. Lett.*, *34*, L06403, doi:10.1029/2006GL028865.

Gibbins, C. N., D. Vericat, R. J. Batalla, and C. M. Gomez (2007a), Shaking and moving: Low rates of sediment transport trigger mass drift of stream invertebrates, *Can. J. Fish Aquat. Sci.*, *64*(1), 1–5.

Gibbins, C. N., D. Vericat, and R. J. Batalla (2007b), When is stream invertebrate drift catastrophic? The role of hydraulics and sediment transport in initiating drift during flood events, *J. Freshwater Biol.*, *52*, 2369–2384.

Haschenburger, J. K., and P. R. Wilcock (2003), Partial transport in a antural gravel bed channel, *Water Resour. Res.*, *39*(1), 1020, doi:10.1029/2002WR001532.

Jackson, W. L., and R. L. Beschta (1982), A model of two-phase bedload transport in an Oregon Coast Range stream, *Earth Surf. Process. Landforms*, *7*, 517–527.

Kellerhals, R., and D. I. Bray (1971), Sampling procedures for coarse fluvial sediments, *J. Hydraul. Div., Am. Soc. Civ. Eng.*, *97*(HY8), 1165–1180.

Lane, E. W., and E. J. Carlson (1953), Some factors affecting the stability of canals constructed in coarse granular materials, in *Proceedings of the 5th Congress International Association for Hydraulic Research, Minneapolis, Minnesota*, 1–4 Sept., 37–48.

Laronne, J. B., C. Garcia, and I. Reid (2001), Mobility of patch sediment in gravel-bed streasm: Patch character and its implications for bedload, in *Gravel Bed Rivers V*, edited by M. P. Mosley, pp. 249–289, New Zealand Hydrological Society, Wellington, N. Z.

Limerinos, J. T. (1970), Determination on the Manning coefficient from measured bed roughness in natural channels, U.S. Geological Survey Water Supply Paper 1898-B, Washington, D. C.

Meyer-Peter, E., and R. Müller (1948), Formuales for bed-load transport, in *Proceedings, 2nd Meeting*, *IAHR*, Stockolm, Sweden, pp. 39–64.

Mosley, M. P., and D. S. Tindale (1985), Sediment variability and bed material sampling in gravel-bed rivers, *Earth Surf. Process. Landforms*, *10*, 465–482.

Müller, E. N., R. J. Batalla, A. Bronstert, and C. Garcia (2008), Modelling bedload transport rates during small floods in a gravel-bed river, *J. Hydraul. Eng.*, *134*(10), 1430–1439.

Neill, C. R. (1968), A re-examination of the beginning of movement of coarse granular bed material, *Rep. No. INT 68*, Hydraulics Research Station, Wallingford, England.

Parker, G., P. C. Klingeman, and D. G. McLean (1982), Bedload and size distribution in paved gravel bed streasm, *J. Hydraul. Div. ASCE*, *108*, 544–571.

Reid, I., J. T. Layman, and L. E. Frostick (1980), The continuous measurement of bedload discharge, *J. Hydraul. Res.*, *18*, 243–249.

Robert, A., A. G. Roy, and B. Deserres (1992), Changes in velocity profiles at roughness transitions in coarse grained channels, *Sedimentology*, *39*(5), 725–735.

Ryan, S. E., L. S. Porth, and C. A. Troendle (2002), Defining phases of bedload transport using piecewise regression, *Earth Surf. Process. Landforms*, *27*, 971–990.

Shields, A. (1936), *Anwendung der Ahnlichkeitsmechanik und der Turbulenzforschung auf die Geschiebebewegung*, Mitt. Preussichen Versuchsanstalt für Wasserbau und Schiffbau, Berlin.

Sutherland, A. J. (1992), Hiding function to predict self armoring, Proc. Int. Association of Hydraulic, Research Int. Grain Sorting Seminar, edited by M. Jaeggi and R. Hunziker, Mitteilungen der Versuchsanstalt für Wasserbau, Hydrologie und Glaziologie No. 117, ETH, Zurich, Switzerland.

Vericat, D., M. Church, and R. J. Batalla (2006), Bedload bias: Comparison of measurements obtained using two (76 and 152 mm) Helley-Smith samplers in a gravel-bed river, *Water Resour. Res.*, *42*, W01402, doi:10.1029/2005WR004025.

Vericat, D., R. J. Batalla, and C. N. Gibbins (2007), Developing stream ecogeomorphology: A new tool to study links between sediment transport and invertebrate drift, *Eos Trans. AGU*, *88*(11), 410.

Wathen, S. J., R. I. Ferguson, T. B. Hoey, and A. Werritty (1995), Unequal mobility of gravel and sand in weakly bimodal river sediments, *Water Resour. Res.*, *31*(8), 2087–2096.

White, R. W., and T. J. Day (1982), Transport of graded gravel bed material, in *Gravel-Bed Rivers*, edited by J. C. Hey, J. C. Bathurst, and C. R. Thorne, pp. 181–223, John Wiley, New York.

Whiting, P. J., and W. E. Dietrich (1990), Boundary shear stress and roughness over mobile alluvial beds, *J. Hydraul. Eng.*, *116*, 1495–1511.

Whiting, P. J., and W. E. Dietrich (1991), Convective accelerations and boundary shear-stress over a channel bar, *Water Resour. Res.*, *27*(5), 783–796.

Wiens, J. A. (1976), Population responses to patchy environments, *Annu. Rev. Ecol. Syst.*, *7*, 81–120.

Wilcock, P. R. (1992), Experimental investigation of the effect of mixture properties on transport dynamics, in *Dynamics of Gravel Bed Rivers*, edited by P. Billi et al., pp. 109–139, John Wiley, New York.

Wilcock, P. R., and B. W. McArdell (1993), Surface-based fractional transport rates: mobilization thresholds and partial transport of sand-gravel sediment, *Water Resour. Res.*, *29*(4), 1297–1312.

Wilcock, P. R., and B. W. McArdell (1997), Partial transport of a sand/gravel sediment, *Water Resour. Res.*, *33*, 235–245.

Wittenberg, L. (2002), Structural patterns in coarse gravel river beds: Typology, survey and assessment of the role of grain size and river regime, *Geogr. Annal.*, *84A*(1), 25–37.

Wolman, M. G. (1954), A method of sampling coarse bed material, *Eos Trans. AGU*, *35*, 951–956.

R. J. Batalla, Department of Environment and Soil Sciences, University of Lleida, Av. Alcalde Rovira Roure, E-25198 Lleida, Catalonia, Spain. (rbatalla@macs.udl.cat)

C. N. Gibbins, Department of Geography and Environment, University of Aberdeen, Elphinstone Road, Aberdeen AB24 3UF, UK. (c.gibbins@abdn.ac.uk)

D. Vericat, Centre for Catchment and Coastal Research, Institute of Geography and Earth Sciences, Aberystwyth University, Llandinam Building, Penglais Campus, Aberystwyth, Wales, Ceredigion SY23 3DB, UK. (ddv@aber.ac.uk)